

Electronic Supplementary Information

Crystallographic Orientation Propagation in Metal Halide Perovskite Thin Films

Alexander Z. Chen, Benjamin J. Foley, Jennifer H. Ma, Matthew R. Alpert, J. Scott Niezgoda, and Joshua J. Choi*

Table of Contents

Experimental Procedures	2
Perovskite film preparation and MACl treatment.....	2
Solar cell fabrication and characterization.....	2
GIXS of perovskite films.....	3
Results from MACl treatment on different MAPbI ₃ film thickness	3
Diffraction pattern of methylammonium chloride.....	3
Comparing intermediate structure of thin and thick perovskite films during MACl treatment	4
GIWAXS patterns of perovskite films with various salt treatment.....	5
MACl treatment on perovskite film on TiO ₂ substrate.....	5
Comparison of solar cell performance with or without MACl treatment	6
SEM images of MAPbI ₃ films before and after MACl treatment.....	6
References	6

Experimental Procedures

Perovskite film preparation and MACl treatment.

Randomly oriented perovskite films with different thickness on glass substrates were fabricated using various methods from the literature^[1,2]. For example, lead iodide (PbI₂, Sigma, 99%) and methylammonium iodide (MAI, Dyesol) at 1:1 molar ratio were dissolved in anhydrous Dimethylformamide (DMF, Sigma) at various concentration from 0.2 M to 1 M. The precursor solution was spin-coated at 4000 rpm and 200 μ L toluene was dropped on the slide during spinning. The slides were then heated on a hot plate to fully crystallize the perovskite film. The MACl treatment was performed by spin-coating a 4 mg/ml methylammonium chloride (MACl)/isopropanol (IPA) solution at 2000 rpm, followed by a brief annealing at 150 °C for 30 seconds. The fabrication of mixed halide slides was adapted from previous papers in the literature^[3,4], by spin-coating a precursor solution that contains 0.8 M PbCl₂ and 2.4M MAI in DMF solvent, followed by annealing at 120 °C. The thickness of films was measured with an atomic force microscope.

Solar cell fabrication and characterization.

Pre-patterned Indium tin oxide (ITO) substrates were cleaned sequentially in detergent solution, DI water and ethanol with ultrasonication, followed by UV-Ozone treatment for 10 minutes. A compact TiO₂ layer was deposited by spincoating 0.15 M titanium diisopropoxide bis(acetylacetonate) in IPA and annealing at 500 °C. Then the slides were transferred into a nitrogen-filled glovebox for perovskite deposition. Deposition of the perovskite active layer was adopted from a previous publication^[2]. A solution containing equimolar lead iodide (PbI₂) and dimethyl sulfoxide (DMSO) at 1 M with DMF as solvent was spin-coated on top of the substrate at 2000 rpm for 60 seconds. Then 51 mg/ml MAI dissolved in IPA was spin-coated at 2000 rpm for 60 seconds. The slides were then annealed at 110 °C for 12 minutes to form a perovskite layer. For MACl treated devices, the same MACl treatment steps described above were performed. The high annealing temperature of 150 °C was found to be necessary for achieving higher performance. For control devices, no MACl treatment was performed. Hole transporting layer solution was prepared by dissolving 72 mg 2,2',7,7'-tetrakis(N,N-dip-methoxyphenylamine)-9,9'-spirobifluorene (Spiro-OMeTAD, Lumtec) in 1 ml chlorobenzene, then 28.8 μ L 4-tert-Butylpyridine and 17.5 μ L 0.52 g/mL bis(trifluoromethane) sulfonimide lithium salt (Li-TFSI, Sigma) acetonitrile solution were added as dopants. The hole transporting layer (HTL) was prepared by spin-coating this solution at 4000 rpm for 30 s. The devices were stored in dry air overnight to oxidize the HTL, then 60 nm Ag was thermally evaporated at 10⁻⁶ Torr vacuum with a shadow mask. 30 cells with MACl treatment and the same number of control devices were fabricated and characterized under simulated AM 1.5G 100 mW/cm² sunlight calibrated with a NREL traceable Si reference cell (PV measurement). An optical mask was used to minimize illuminating the non-device area of the sample. Each solar cell has an active area of 0.03 cm² defined by the overlap between metal electrode and ITO layer.

GIXS of perovskite films.

Grazing-Incidence X-ray Scattering (GIXS) was performed at D-1 beamline at the Cornell High Energy Synchrotron Source (CHESS), with a temperature-controllable sample stage. The X-ray wavelength is 0.1162 nm and incident angle of the beam upon the sample was 0.25°. A Pilatus 200k detector was placed at 163.185 mm from the sample. For *in-situ* measurements, the sample was moved to a new position after each measurement to minimize X-ray induced damage. The collected images have a horizontal black stripe which is due to a detector gap. The following MAPbI₃ unit cell parameters were used to fit the preferential orientation of measured films: cubic, $a=b=c=0.62$ nm, $\alpha=\beta=\gamma=90^\circ$; tetragonal, $a=b=0.89$ nm, $c=1.23$ nm, $\alpha=\beta=\gamma=90^\circ$. The simulation of GIXS peak position was done by in-house software package.

Results from MACI treatment on different MAPbI₃ film thickness

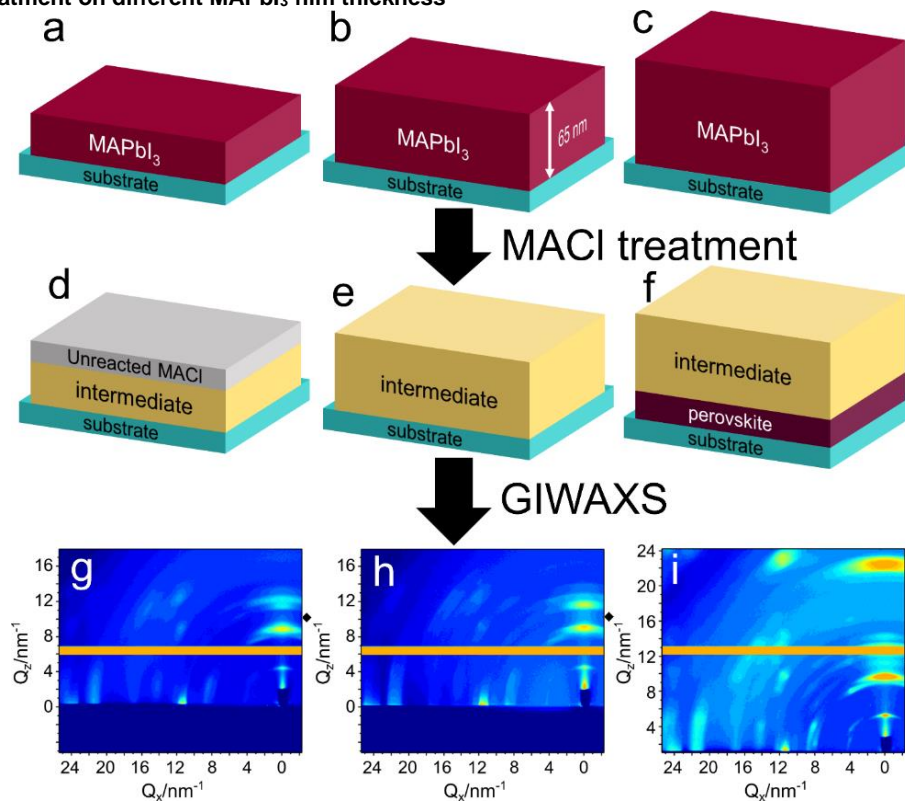


Figure S1. Measurement of the thickness of MAPbI₃ film reacting with MACI during MACI treatment. MAPbI₃ films with different thicknesses were made by varying precursor solution concentration of solvent-solvent extraction method from 0.2 M to 0.7M (a–c), on which MACI treatment was performed (d–f). GIWAXS patterns were then collected with the treated films (g–i), with the Q position of MAPbI₃ (110) peak labelled with ◆. The perovskite peak started to appear when the precursor concentration is ≥ 0.3 M, corresponding to a thickness ≥ 65 nm, as measured by atomic force microscopy.

Diffraction pattern of methylammonium chloride

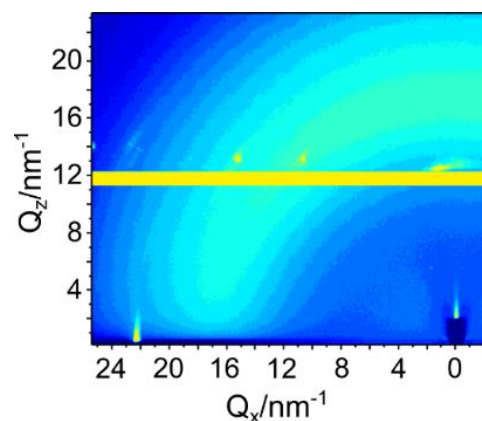


Figure S2. GIWAXS pattern of methylammonium chloride with a glass slide as substrate.

Comparing intermediate structure of thin and thick perovskite films during MACI treatment

By analyzing the intermediate GIWAXS pattern of thin (Fig. 2(b)) and thick (Fig. 3(b)) perovskite film, it was found out that the thick film intermediate pattern can be reproduced by super-positioning the patterns of an oriented thin intermediate and a randomly oriented thick perovskite film. The oriented component of the superposition indicates an anisotropic formation of the intermediate species. The image manipulation was performed in Matlab.

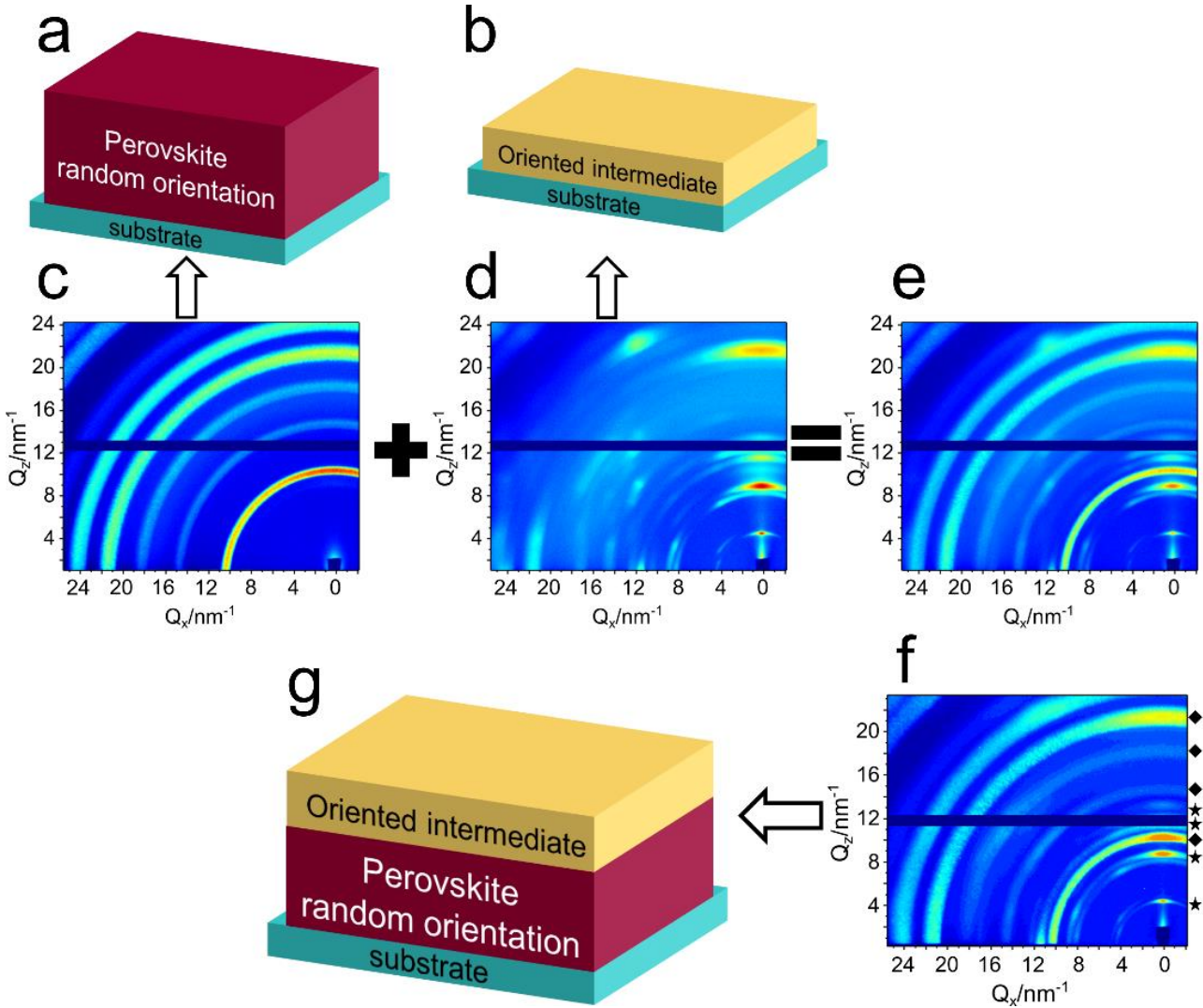


Figure S3. Summing the GIWAXS patterns of a randomly oriented thick perovskite (a, c) and a thin perovskite oriented intermediate (b, d) yields a matching result (e) for thick intermediate pattern (f), which has a proposed structure of a top oriented intermediate layer and a bottom randomly oriented perovskite layer. The peaks labelled by stars (★) has an oriented structure, while perovskite peaks labelled by diamonds (◆) has a mostly random orientation.

GIWAXS patterns of perovskite films with various salt treatment

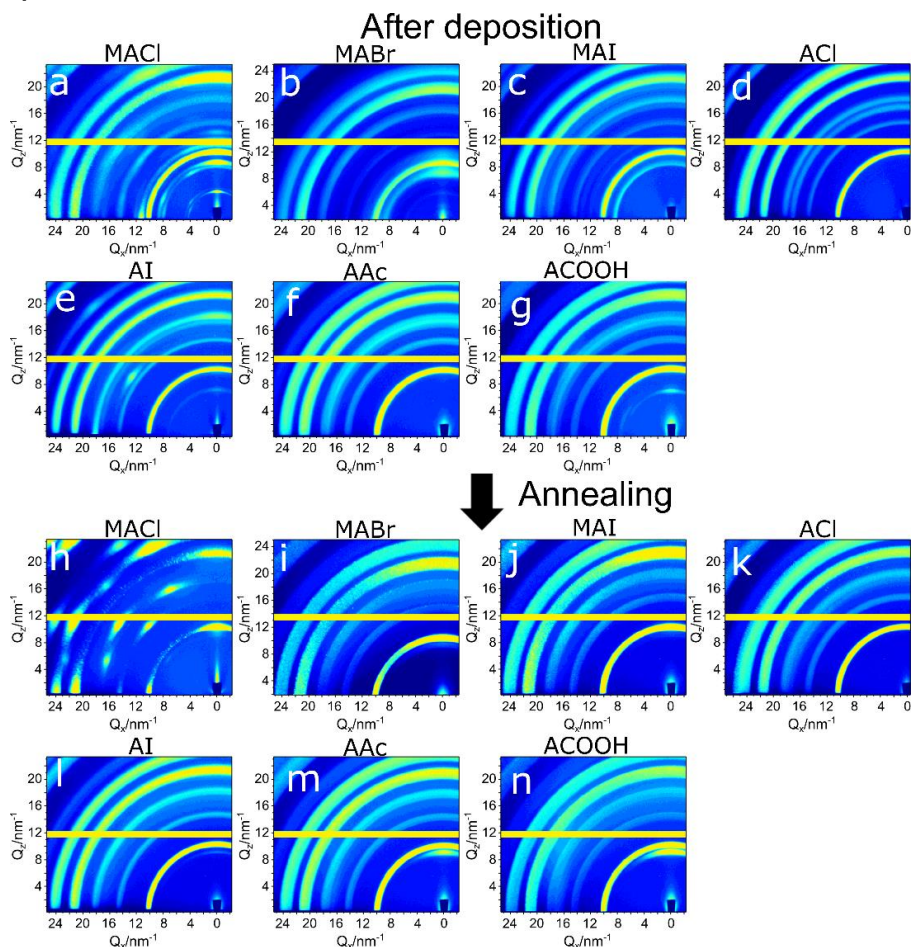


Figure S4. GIWAXS patterns of perovskite films with various salt treatment. Starting from MAPbI_3 with random orientation (a), the films were treated with various salts other than MACI, including methylammonium bromide (MABr), methylammonium iodide (MAI), ammonium chloride (ACI), ammonium iodide (AI), ammonium acetate (AAc) and ammonium formate (ACOOH).

MACI treatment on perovskite film on TiO_2 substrate

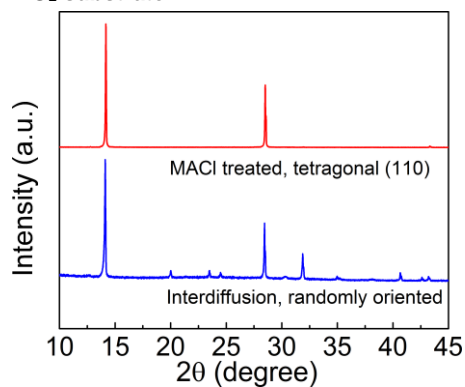


Figure S5. XRD of MAPbI_3 films prepared by interdiffusion method² on TiO_2 substrates and films with the same preparation method followed by MACI treatment.

Comparison of solar cell performance with or without MACl treatment

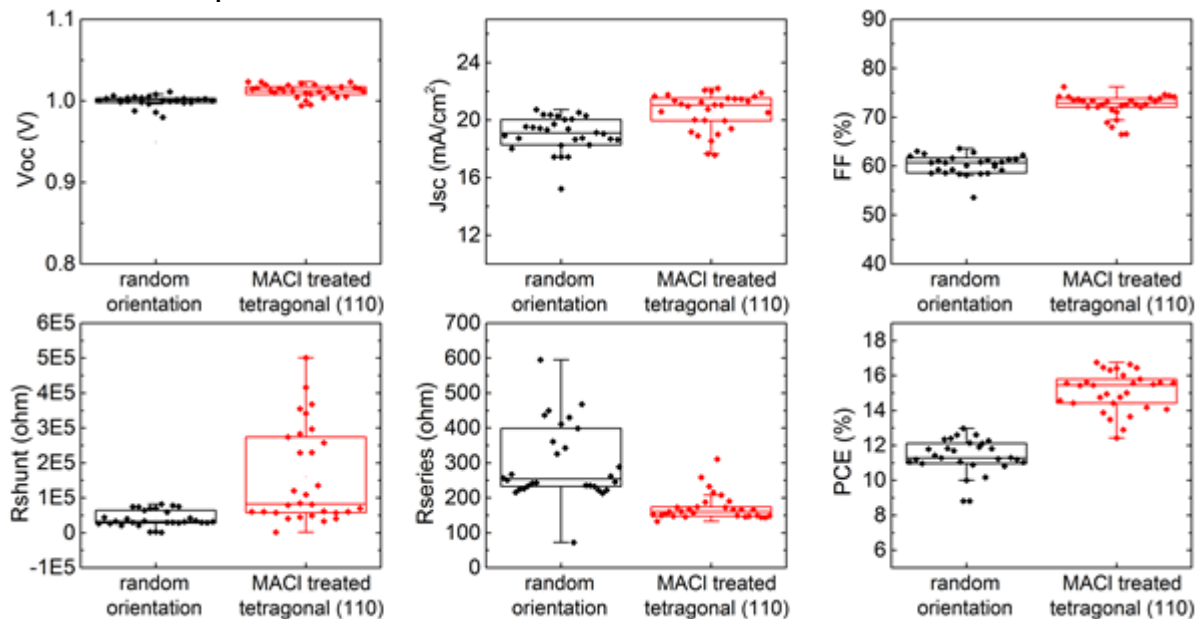


Figure S6. Detailed device parameters of solar cells made with MACl treatment and control devices.

SEM images of MAPbI₃ films before and after MACl treatment

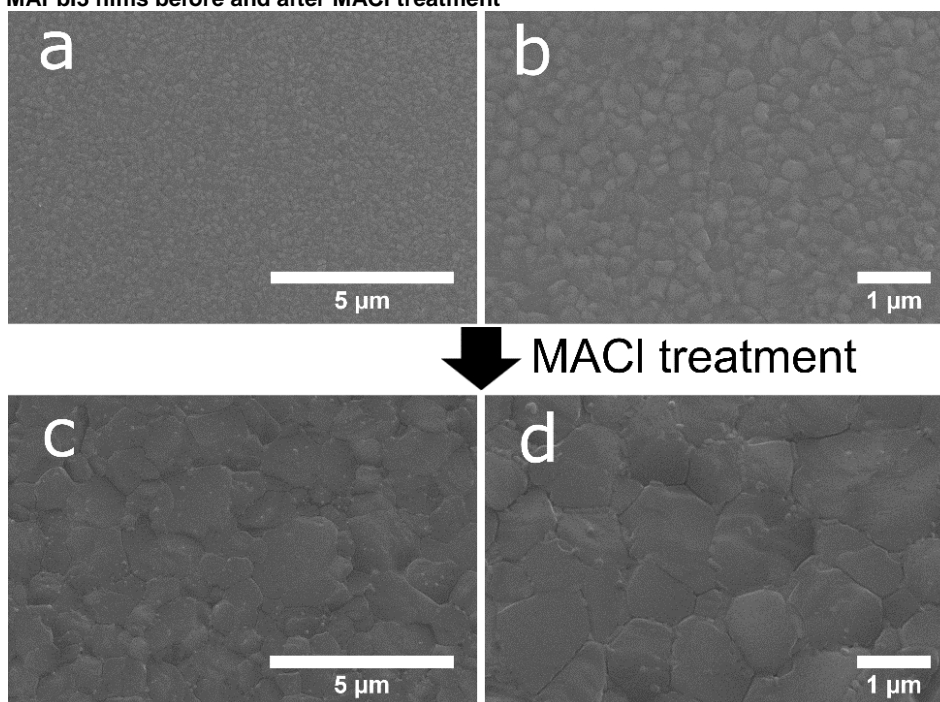


Figure S7. SEM of MAPbI₃ films prepared by interdiffusion method on TiO₂ substrates (a, b) and films with the same preparation method followed by MACl treatment (c, d).

References

- [1] Y. Zhou, M. Yang, W. Wu, A. L. Vasiliev, K. Zhu, N. P. Padture, *J. Mater. Chem. A* **2015**, 3, 8178-8184.
- [2] H. Zhou, Q. Chen, G. Li, S. Luo, T. B. Song, H. S. Duan, Z. Hong, J. You, Y. Liu, Y. Yang, *Science* **2014**, 345, 542-546.
- [3] S. D. Stranks, G. E. Eperon, G. Grancini, C. Menelaou, M. J. Alcocer, T. Leijtens, L. M. Herz, A. Petrozza, H. J. Snaith, *Science* **2013**, 342, 341-344.
- [4] Q. Dong, Y. Yuan, Y. Shao, Y. Fang, Q. Wang, J. Huang, *Energy Environ. Sci.* **2015**, 8, 2464-2470.